

Electron paramagnetic resonance of a platinum pair complex in silicon

M. Höhne

Institut für Kristallzüchtung, Rudower Chaussee 6, D-O-1199 Berlin, Federal Republic of Germany

(Received 29 October 1991)

EPR measurements of hydrogen-treated Si:Pt single crystals reveal a pair of equivalent Pt ions on next-nearest-neighbor sites. The g values and hyperfine parameters differ essentially from those of a previously detected Pt pair center; therefore, an additional constituent in at least one of the complexes is suggested. Possible models with adjacent defects having spin states of $S=0$ or $\frac{1}{2}$, respectively, are offered.

INTRODUCTION

In 1988 von Bardeleben *et al.*¹ detected a paramagnetic defect in Pt-doped Si, which revealed the hyperfine structure (hfs) corresponding to two equivalent Pt ions on a $\langle 110 \rangle$ axis. That defect will be called a type-I defect in this paper. The g values were $g_x=1.5181$, $g_y=2.1869$, and $g_z=1.6317$ with $x \parallel [110]$, $y \parallel [\bar{1}10]$, and $z \parallel [001]$, and the hyperfine parameters were $A_\xi=256$ MHz, $A_\eta=156$ MHz, and $A_\zeta=207$ MHz with $\xi \parallel [1\bar{1}1]$, $\eta \sim [110]$, and $\zeta \sim [\bar{1}12]$. The orthorhombic symmetry of the center was in accordance with the incorporation of the pair into the Si matrix; therefore no additional constituent of the paramagnetic complex had to be assumed. An earlier report² on a pair of two nonequivalent Pt ions in Si turned out³ to be erroneous.

It will be shown in this paper that another defect containing two equivalent Pt ions on a $\langle 110 \rangle$ axis can be produced. This defect will be called a type-II defect in this paper. Also in this case the hfs does not give any hint at additional constituents. Therefore no final statement concerning the model can be given; but the conditions of sample preparation might suggest the presence of hydrogen in the complex defect.

EXPERIMENT

The starting material was n -type Si with $3 \times 10^{16} \text{ cm}^{-3}$ P. Pt was diffused at 1200°C for several days; consequently a concentration of approximately $1 \times 10^{17} \text{ cm}^{-1}$ could be assumed. The diffusion was finished by retarded quenching.⁴ The quenching to room temperature was interrupted for a time less than a minute in the range of 900°C .

The samples were then prepared in a conventional hydrogen-containing rf-glow discharge at 300°C for 30 min; the EPR measurement at 20 K did not show a relevant Pt-related spectrum; isolated Pt defects are detected only at lower temperature.⁵ A subsequent anneal for 30 min at 360°C produced the defect, which is the subject of this paper. Its concentration may be estimated from the EPR spectra to be roughly 10^{14} cm^{-3} .

The defect discussed here was also produced by an alternative preparation. Surface reactions in an acid atmo-

sphere at high temperatures introduces—depending on subsequent processing—several complex defects,⁶ and among them the type-II pair complex was formed in a comparable concentration.

The EPR measurements were done in X band at 20 K. The orientation of the samples was improved *in situ* in the beginning of the EPR experiments.

EXPERIMENTAL RESULTS

The angular dependence of the spectra for rotating the sample in a $\{110\}$ plane was investigated. The analysis could be performed in a spin $S=\frac{1}{2}$ system. The symmetry of the defect was clearly orthorhombic corresponding to the Zeeman part of the spin Hamiltonian:

$$\mathcal{H}_{Ze} = \beta(g_x S_x B_x + g_y S_y B_y + g_z S_z B_z) \quad (1)$$

with the directions of the x , y , and z axes defined above and the parameters

$$g_x=2.1631, \quad g_y=2.1107, \quad \text{and} \quad g_z=2.1755.$$

The symbols have the usual meanings; β is the Bohr magneton.

The only isotope of Pt with nonzero nuclear spin $I=\frac{1}{2}$ is ^{195}Pt with a natural abundance of 0.338. Therefore the probability to find both of the nuclei with $I=0$ is 0.438, it is 0.448 to find only one of them with $I=\frac{1}{2}$, and it is 0.114 for $I=\frac{1}{2}$ on both nuclei. For orientations where the two Pt ions are not only geometrically, but also magnetically equivalent, one would therefore expect five hyperfine components of the corresponding line group with a ratio of intensities near to 1:8:18:8:1.

Figure 1 shows the EPR spectrum for a direction of the magnetic field nearly parallel with a $\langle 100 \rangle$ crystal axis ($\mathbf{B} \parallel \langle 100 \rangle$). In this case the hyperfine components of both line groups exhibit the ratio of intensities calculated above. The sample had been slightly misoriented intentionally in order to demonstrate the double intensity of the high-field line group [corresponding to $g=(g_x^2+g_y^2)^{1/2}$] compared to the low-field group (g_z).

For $\mathbf{B} \parallel \langle 110 \rangle$ the spectrum is shown in Fig. 2. Only the high-field group (g_y) clearly makes the characteristic ratio of intensities obvious. The overlapping low-field

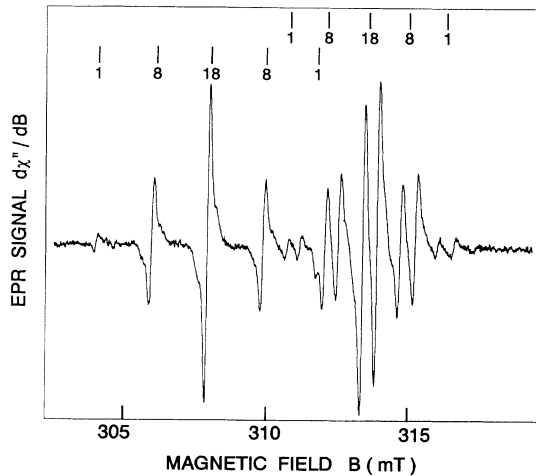


FIG. 1. EPR spectrum at 20 K for nearly $\mathbf{B} \parallel \langle 100 \rangle$. Positions and relative intensities of hfs groups due to two magnetically equivalent Pt ions are indicated.

groups can be simulated in accordance with the following theoretical description.

The whole angular dependence could be represented by (1) and a hyperfine part of the spin Hamiltonian

$$\mathcal{H}_{\text{hf}} = \sum_{j=1}^2 (A_{\xi} S_{\xi_j} I_{\xi_j} + A_{\eta} S_{\eta_j} I_{\eta_j} + A_{\zeta} S_{\zeta_j} I_{\zeta_j}). \quad (2)$$

Index $j=1,2$ relates to the Pt nuclei, each of which has its own system of fundamental axes ξ_j, η_j, ζ_j for the hyperfine interaction. The axes η_1 and η_2 coincide with the y axis, whereas the axes ξ_1 and ξ_2 are inclined by $\rho_1 = +29^\circ$ and $\rho_2 = -29^\circ$, or vice versa, with respect to the z axis. The possible arrangements are sketched in Fig. 3 in a plane normal to $y \parallel \eta$. The parameters, equal for both Pt ions, are

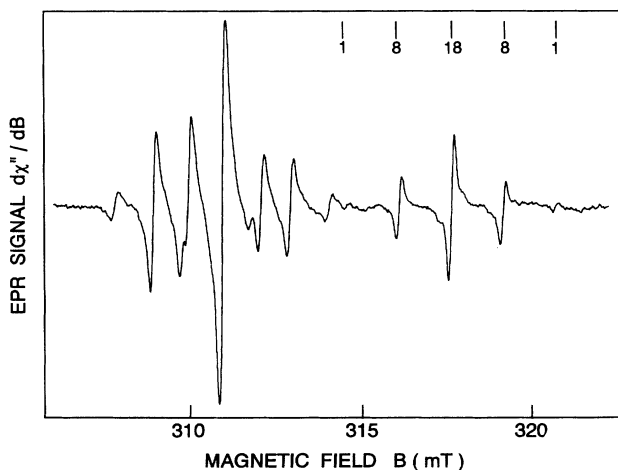


FIG. 2. EPR spectrum at 20 K for $\mathbf{B} \parallel \langle 110 \rangle$. Positions and relative intensities of a hfs group due to two magnetically equivalent Pt ions are indicated.

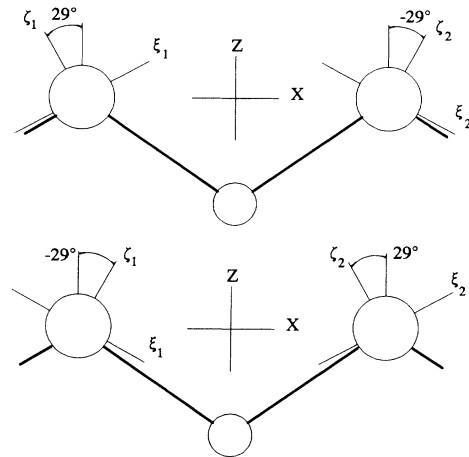


FIG. 3. Two possible orientations of g -tensor and hfs-tensor fundamental axes perpendicular to the $y \parallel \eta$ axis in the silicon lattice.

$$|A_{\xi}| = 9 \times 10^{-4} \text{ cm}^{-1},$$

$$|A_{\eta}| = 30 \times 10^{-4} \text{ cm}^{-1},$$

$$|A_{\zeta}| = 43 \times 10^{-4} \text{ cm}^{-1}.$$

For comparison we repeat the parameters quoted above for the type-I defect¹ in the same units:

$$|A_{\xi}| = 85 \times 10^{-4} \text{ cm}^{-1},$$

$$|A_{\eta}| = 52 \times 10^{-4} \text{ cm}^{-1},$$

$$|A_{\zeta}| = 69 \times 10^{-4} \text{ cm}^{-1}.$$

One has to keep in mind that the axes ξ and ζ may slightly differ for the type-I and the type-II defects, respectively. In the first case, $\xi \sim [1\bar{1}1]$ had been reported,¹ which would correspond to $|\rho_1| = |\rho_2| \sim 35^\circ$.

Furthermore one should be aware of the fact that in spite of the overall orthorhombic symmetry of the defect, each of the Pt ions sees an environment of lower symmetry. Thus actually the components of the hfs matrix cannot be inferred from the experiment.⁷ In determining the hfs parameters we assume that the hfs can approximately be described by a matrix of rhombic symmetry, which has tacitly been done also for the type-I defects.¹

According to the values of the parameters, second-order terms could be neglected here in describing the line positions within the limits of error. The line positions were calculated from

$$B = \frac{h\nu}{g\beta} - \frac{1}{g\beta} (K_1 m_1 + K_2 m_2). \quad (3)$$

The microwave frequency ν was measured by a frequency meter and calculated from the positions of the phosphorus lines. The quantum numbers m_1 and m_2 for the nuclear-spin components may be $\pm \frac{1}{2}$ for ¹⁹⁵Pt or 0 for the other isotopes, corresponding to the probabilities mentioned above. With θ and δ as the usual angles defining the direction of the magnetic field with respect to the g -tensor axes one obtains with (1) and (2)

$$K_j = \frac{1}{g} [A_\xi^2 (\cos \rho_j g_x \sin \delta \sin \theta + \sin \rho_j g_z \cos \theta)^2 + A_\eta^2 g_y^2 \cos^2 \delta \sin^2 \theta + A_\xi^2 (-\sin \rho_j g_x \sin \delta \sin \theta + \cos \rho_j g_z \cos \theta)^2]^{1/2} \quad (j = 1, 2). \quad (4)$$

It is evident from (4) that the quantity K_j is independent of the sign of ρ_j only for certain values of θ and δ ; only for these angles are the two Pt ions magnetically equivalent.

The line positions versus the angle between the magnetic field \mathbf{B} and the $\langle 100 \rangle$ direction in the plane of rotation were calculated for the possible orientations of the orthorhombic defect in the lattice. This angular dependence is shown in Fig. 4. Bold lines represent the positions of EPR lines resulting from a pair of nuclei with zero spin ($m_1 = m_2 = 0$). Of course they are the most intense lines, which simply follow the dependence of the g values. The medium lines arise from pairs with one spin $I = 0$ and one spin $I = \frac{1}{2}$ ($m_1 = \pm \frac{1}{2}, m_2 = 0$, or vice versa). The bold lines and the intermediate ones exactly reflect the experimental data, which were recorded in a dense sequence of angles of rotation. Therefore we omitted the drawing of single experimental points. Resonances corresponding to the thin dotted lines ($m_1 = \pm \frac{1}{2}, m_2 = \pm \frac{1}{2}$) were covered by noise in most cases because of the small probability for finding nonzero spin on both nuclei; they were detected only for certain directions as those, represented in Figs. 1 and 2. Even details of those spectra are in agreement with Fig. 4: the splitting of the high-field group in Fig. 1 due to the small misalignment of \mathbf{B} and $\langle 110 \rangle$ and the superposition of the low-field line groups for $\mathbf{B} \parallel \langle 110 \rangle$.

Figure 4 visualizes correctness and reliability of the spin Hamiltonian and its parameters. Especially the hyperfine replica of the bold lines split in a way which

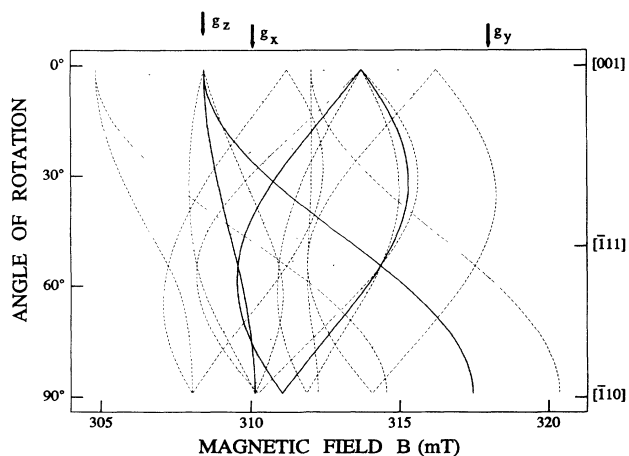


FIG. 4. Angular dependence of the EPR spectra calculated according to the spin Hamiltonian of this paper. Bold lines and medium ones reflect a dense sequence of experimental points; resonances corresponding to thin dotted lines are mostly covered by noise (but detected in Figs. 1 and 2).

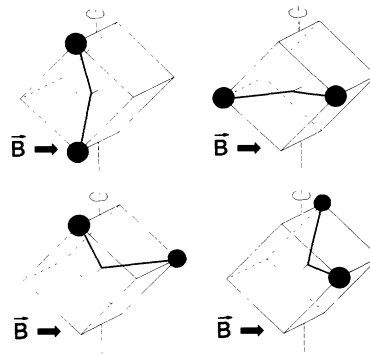


FIG. 5. The four orientations of pair complexes with respect to magnetic field \mathbf{B} and $\langle 110 \rangle$ axis of rotation (broken vertical line). Bold lines indicate the hyperfine ξ axes.

corresponds to (4) and to the geometrical imagination of rotating a crystal about a $\langle 110 \rangle$ axis of rotation: The four possible arrangements of the defect in the lattice are sketched in Fig. 5, and it is obvious that only for one type (left-hand side) the two Pt ions are equivalent with respect to the magnetic field \mathbf{B} for any angle of rotation. All the arrangements yield magnetic equivalence for $\mathbf{B} \parallel \langle 100 \rangle$, and both upper two do it for $\mathbf{B} \parallel \langle 110 \rangle$.

The spectra were observed after cooling the samples in the dark, whereas the EPR lines due to the phosphorus were detected only under band-gap light. The spectrum of the type-II complex was scarcely influenced by the light.

DISCUSSION

A doubtless conclusion from this investigation is the formation of another $\langle 110 \rangle$ -oriented pair of equivalent Pt ions in a defect, which differs essentially in the parameters of the spin Hamiltonian from the previously detected type-I defect.¹ The existence of two different "pairs" makes the assumption of isolated pairs doubtful, though neither symmetry arguments nor hfs point at other constituents of the complex defects.

The idea of different pair configurations, which were detected and thoroughly investigated in the case of iron-acceptor pairs,⁸⁻¹⁰ is scarcely promising for the Pt-Pt pair defects of type I and II, because the symmetry of both complexes is equal.

Two models are proposed in Fig. 6. The preparation conditions of the type-II defect might suggest the assumption of a hydrogen-related defect. Thus in (a) the $S = 0$ defect might be a hydrogen molecule near an interstitial T_d site, which is the natural site for electrically and optically inactive hydrogen in silicon.¹¹ Consequently no interaction of the paramagnetic state with hydrogen nuclei is expected, which agrees with the lack of hfs in the spectra.

Possibly the retarded quenching favors the formation of Pt-Pt pairs, and the annealing at 360°C might yield the complexing of hydrogen or other defects with the pairs. One might suppose that the isolated pairs of paramagnetic Pt ions are spin compensated. The complexing with

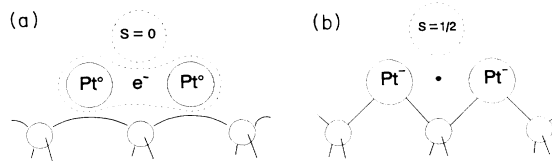


FIG. 6. (a) Model variant for the type-II complex: Two Pt ions near NNN substitutional sites with one common negative charge; another defect with $S=0$ near an adjacent tetrahedral interstitial site. (b) Other possible model: Two Pt^- ions near NNN substitutional sites and another paramagnetic defect ($S = \frac{1}{2}$) between a C site (denoted by a dot) and a tetrahedral interstitial site T_d .

other defects may create levels in the gap related to once negatively charged defects. A molecular-orbital (MO) treatment would in this case be near the vacancy model.¹² All the neighboring silicon bonds are reconstructed. Of course contrary to this rough picture and in agreement with refined theoretical treatments,¹³ the MO function must include symmetry-adapted sp ligand orbitals besides the $5d$, $6s$, and $6p$ orbitals of the Pt ions. Such a procedure had been recommended for $5d^n$ complexes in Si.¹⁴ In the case of the type-II defects the ligand hfs is only slightly indicated by narrow tails of the resonance lines (see Figs. 1 and 2), compatible with a weak coupling to the lattice.

Another way of explaining a paramagnetic state in the sense of model (a) in Fig. 6 would combine a Pt^- ion and a Pt^0 atom, which in the limiting case of mixed valence states with intervalence charge transfer of sufficiently high frequency between strongly interacting ions yields two completely equivalent ions.¹⁵

The g shifts are compatible with the thorough treatment of the electronic structure of Pt in Si.¹⁶ A physical reason for the nearly isotropic g matrix of the type-II defect contrary to the type-I defects has not been given up

to now.

A second model, indicated in (b) of Fig. 6, attributes the experimental spectrum to a $-\frac{1}{2} \leftrightarrow +\frac{1}{2}$ transition of three exchange-coupled $S = \frac{1}{2}$ spins due to two Pt^- ions and an unknown defect. The Pt^- ions would have bonds with only two Si ligands.¹⁶ In this case one has to keep in mind that g matrices and A matrices of the constituents cannot be inferred simply from the experiment, which was demonstrated, for example, in the case of other Pt-related complexes.¹⁷

Evidently this model would hold only if the unknown constituent is not hydrogen, because contrary to the experimental result one should expect a distinct hfs caused by a paramagnetic state of a hydrogen atom.

CONCLUSIONS

Another pair of two equivalent Pt ions in $\langle 110 \rangle$ coordination has been clearly detected. It is of the same type of symmetry as another one that has previously been reported. Though neither hyperfine interactions nor symmetry arguments demand the assumption of a third constituent, its existence in at least one of the two Pt-Pt complex defects is strongly suggested. The conditions of sample preparation hint at the possibility of a hydrogen molecule near the Pt-Pt pair, but also alternative neighboring defects or even the identification of the additional defects with an isolated Pt-Pt pair cannot be excluded.

ACKNOWLEDGMENTS

The author is greatly indebted to W. Gehlhoff and K. Irmscher for critical discussions. The investigation has greatly profited from committed and patient assistance in sample preparation by U. Juda. I would like to thank U. Rehse for valuable hints concerning data handling and L. Eglinski and H. Fabig for enabling the checking of some variants in sample preparation.

¹H. J. von Bardeleben, D. Stiévenard, M. Brousseau, and J. Barreau, *Phys. Rev. B* **38**, 6308 (1988).

²J. C. M. Henning and E. C. J. Egelmeers, *Phys. Rev. B* **27**, 4002 (1983).

³R. F. Milligan, F. G. Anderson, and G. D. Watkins, *Phys. Rev. B* **29**, 2819 (1984).

⁴M. Höhne, *Solid State Phenom.* **67**, 329 (1989).

⁵G. W. Ludwig and H. H. Woodbury, *Solid State Phys.* **13**, 223 (1962).

⁶M. Höhne and U. Juda (unpublished).

⁷A. Abragam and B. Bleaney, *Electron Paramagnetic Resonance of Transition Ions* (Clarendon, Oxford, 1970).

⁸J. van Kooten, G. A. Weller, and C. A. J. Ammerlaan, *Phys. Rev. B* **30**, 4564 (1984).

⁹W. Gehlhoff, K. Irmscher, and J. Kreissl, in *New Developments in Semiconductor Physics*, edited by G. Ferenczy and B.

Beleznyay, *Lecture Notes in Physics Vol. 301* (Springer-Verlag, Berlin, 1988), p. 262.

¹⁰P. Omling, P. Emanuelsson, W. Gehlhoff, and H. G. Grimmeiss, *Solid State Commun.* **70**, 807 (1989).

¹¹S. J. Pearton, J. W. Corbett, and T. S. Shi, *Appl. Phys. A* **43**, 153 (1987).

¹²G. D. Watkins, *Physica* **117/118B**, 9 (1983).

¹³A. Fazzio, M. J. Caldas, and A. Zunger, *Phys. Rev. B* **32**, 934 (1985).

¹⁴M. Höhne, *Phys. Status Solidi B* **138**, 337 (1986).

¹⁵A. Bencini and D. Gatteschi, *EPR of Exchange Coupled Systems* (Springer-Verlag, Berlin, 1990), p. 42.

¹⁶C. A. J. Ammerlaan and A. B. van Oosten, *Phys. Scr.* **T25**, 342 (1989).

¹⁷M. Höhne and W. Gehlhoff, *Phys. Status Solidi B* **165**, 189 (1991).